PAN ARCHIVES OF ACOUSTICS
Vol. **39**, No. 4, pp. 653–663 (2014)

DOI: 10.2478/aoa-2014-0071

Identification of the Types of Measured Acoustic Modes Inside the Operator's Cab in a Bulldozer

Zygmunt DZIECHCIOWSKI[(1)], Marek S. KOZIEŃ[(2)]

[(1)] *Institute of Machine Design*
[(2)] *Institute of Applied Mechanics*
Cracow University of Technology
Al. Jana Pawła II 37, 31-864 Kraków, Poland; e-mail: {dziechci, kozien}@mech.pk.edu.pl

(*received October 19, 2014; accepted December 5, 2014*)

The aim of the study was to identify acoustic and structural modes in the spectrum obtained experimentally inside an operator's cab in a bulldozer. Measurements were taken inside the operator's cab in a caterpillar-track bulldozer Polremaco TD12NPH2E-2000, designed for work in underground mine enclosures. The acoustic pressure spectrum was obtained for varied rotational speeds of the engine during the free run of the machine. The reverberation time of the cab was determined basing on the pulse-type excited pressure response, followed by identification of the spectral components registered by measurements. Thus, identified frequencies were compared with natural acoustic frequencies registered inside the operator's cab and with frequencies associated with the valves and ignition frequencies due to rotational speed and natural frequencies of structural vibrations of the cab's walls. This study was conducted in an attempt to reduce the noise inside the operator's cab using passive methods.

Keywords: heavy duty machine, acoustic modes, structural modes.

1. Introduction

Bulldozers are a group of widely used heavy duty machines whose operators are exposed to acoustic disturbances and vibrations negatively impacting on humans. In considerations of the cab's design and the operating mode of the machine (and, consequently, the type of acting disturbances), the obtained noise spectrum is mostly of the broadband type (Misun, Svancara, 2001; Nizioł, 1987). The issues associated with noise and vibration reduction in heavy duty machines are addressed in more detail in the works: (Michałowski, 2000; Michałowski, Stolarski, 1998) or in the study concerned with practical applications (Dziechciowski *et al.*, 2001).

In the general case, modelling of an acoustic field inside a cab, whilst the machine is in service, is a difficult task. Problems involved in modelling are addressed elsewhere (Koppman, 1982; Succi, 1987). Widely employed methods of analysing acoustic fields inside the vehicle cabs include the FEM methods (Nefske *et al.*, 1982; Freymann, 1999; Turner, Turgay, 1998) and the boundary element method (Hargreaves, 1998). Due to the complex nature of the analysis, these methods are also recalled to determine the modal characteristic of the cab's interior (Koopman, 1976; Myung-Ho *et al.*, 1993).

A most interesting approach to noise reduction inside the machine operator's cab involves the low-frequency analysis with the use of Helmholtz resonators (Stolarski, 1995; Xiaofeng *et al.*, 2012; Chiu, 2013).

Another vital aspect to be addressed in research aimed at noise reduction inside the cab is the analysis of noise radiated by panel-type vibrating structures such as cab walls (Freymann, 1999; Kozień, Wiciak, 2004; Sung-Hee *et al.*, 2012; Rdzanek, 2002; Rdzanek *et al.*, 2003; Zawieska, Rdzanek, 2006; Zawieska *et al.*, 2007; Szemela *et al.*, 2013). At the further stage, research work is aimed at reducing vibrations of components through the change of the system's geometry (Kozień, Nizioł, 1993; Kozień, Wiciak, 2004) through application of piezoelectric elements attached to specified points on the vibrating elements (Kozień, Wiciak, 2008; 2009; 2010) or through application of specially designed compact micro-perforated membrane absorbers for polycarbonate panels (Min *et al.*, 2013). The knowledge

of the spectral characteristics of the acoustic field inside the cab can be utilised to effectively apply active noise reduction methods is various applications (Nelson, Elliott, 1993; Stoebner, Gaul, 2001). The interesting idea for the noise control of construction machines is proposed in (Carletti, 2013).

Identification of the acoustic field inside the machine operator's cab is a major step in the vibroacoustic analysis (Engel, 2000; Pleban, 2014). Of particular importance is the information about the frequency spectrum of the noise being measured and identification of the types and the sources of particular frequency components. These analyses can be performed in the context of future research work. The author's most far-reaching goal is the reduction of noise levels inside the operator's cab in a bulldozer intended for work in underground mines, in order to improve the acoustic conditions experienced by the operator (Engel, 2000; Kazimierska, Grębosz, 2001). The authors' research efforts are focused on identification of frequency components in the acoustic pressure spectra at the selected points inside the cab, identification of frequencies associated with the motor operation (rotational speed, valve frequency, ignition frequency) and of natural frequencies of selected elements of the cab walls. As the entire cab volume has to be considered in anticipation of the wave phenomena, the analysis is restricted to the low-frequency range, up to 300 Hz. A similar study is reported in the work (Sung-Hee *et al.*, 2012). Certain aspects of the issue being addressed have already been presented at conferences (Dziechciowski, Kozień, 2014a; 2014b).

2. Analysed machine

Measurements were taken inside a operator's cab in a bulldozer Polremaco TD12NPH2E-2000, shown in Fig. 1. The schematic view of the cab is shown in Fig. 2. The machine is powered by a series supercharged compression-ignition engine Cummins QSB 6.7, with six cylinders, four valves per each. The internal dimensions of the investigated operator's cab are $1.3 \times 1.05 \times 1.25$ m (length × width × height). The total surface area of the walls equals 8.82 m^2 and the glass panels occupy 0.98 m^2. The cab is made of steel sheets varying in thickness and reinforced with steel profiles. It is integrated with the machine frame. When connected to the bulldozer frame and covered with a roof structure, the cab becomes a closed volume. The floor in the bulldozer is made of two panels. The interior walls in the cab are covered with the sound-absorbing materials (polyurethane foam covered with perforate fake leather), as shown in Fig. 1b. The remaining surfaces are made of steel sheets varying in thickness and toughened glass (windows). The dimensions of major

a)

b)

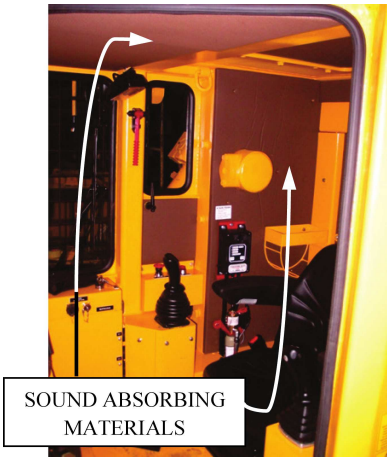

Fig. 1. Bulldozer Polremaco TD12NPH2E-20: a) general view, b) interior).

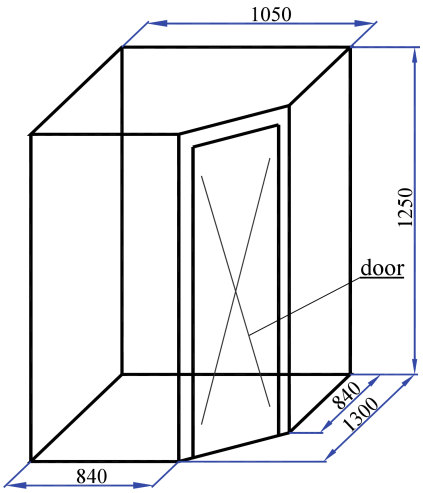

Fig. 2. Schematic view of the operator's cab (internal dimensions).

panels making up the cab are summarised in Table 1, giving also the material specification and the method of fixing. Developed view of cab walls is presented in Fig. 3.

Table 1. Major plates elements in the cab.

Plate No.	Description	Material	Dimensions [mm]	Edge fixing
1	Floor plate 2	Steel 18G2A	1270×400×16	Welded along the perimeter
2	Rear plate	Steel 18G2A	1110×1300×5	Welded along the perimeter
3	Side plate	Steel 18G2A	510×1300×10	Welded along the perimeter
4	Roof opening	Steel 18G2A	647×647×12	Screwed down along the perimeter via a rubber packing
5	Side window – front part	Toughened glass	418×670×5	Fixed on a rubber packing
6	Side window – rear part	Toughened glass	192×390×5	Fixed on a rubber packing
7	Window panel – door	Toughened glass	478×750×5	Fixed on a rubber packing
8	Front window panel	Toughened glass	575×570×5	Fixed on a rubber packing
9	Front panel	Steel 18G2A	840×1250×10	Welded along the perimeter
10	Floor panel 2	Steel 18G2A	1270×400×16	Welded along the perimeter

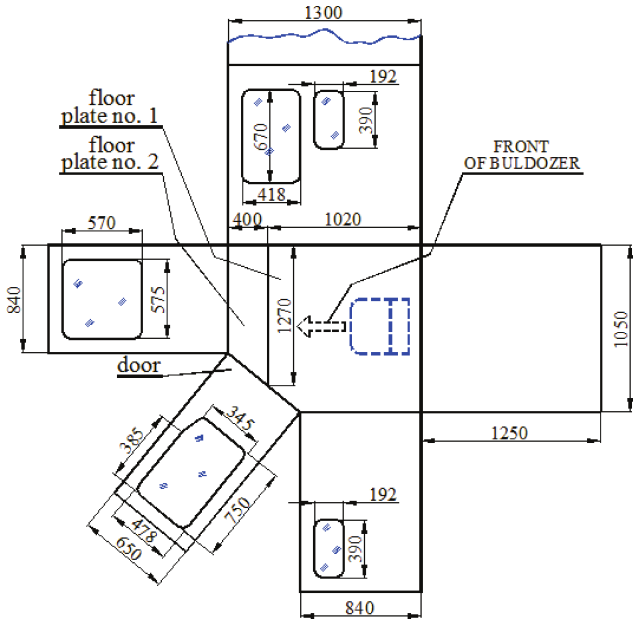

Fig. 3. Developed view of cab walls.

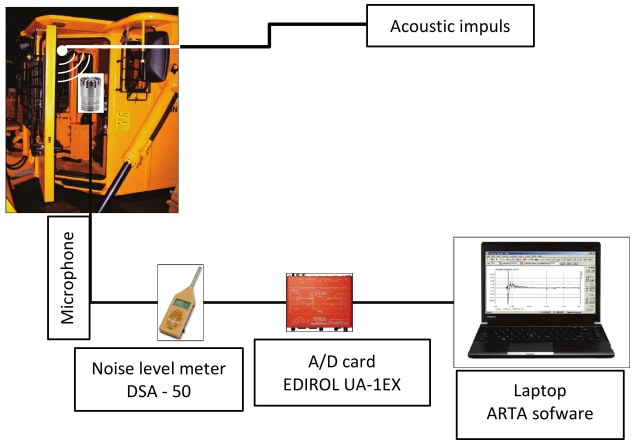

Fig. 4. Equipment for impulse response measurements.

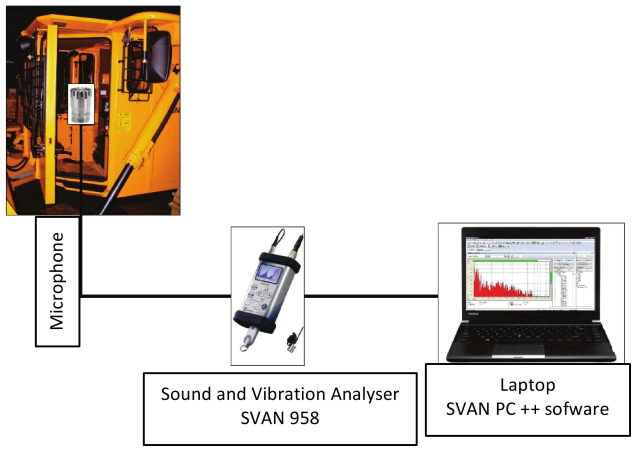

Fig. 5. Equipment for spectral analysis in the service conditions.

3. Measurements and analysis of results

The experimental program included the measurements of:

1. Impulse response of the acoustic volume. The experimental set-up is shown in Fig. 4.
2. Acoustic field response in the service conditions (during the idle run of the engine and for three rotational speeds: 750 rpm, 1600 rpm, 2300 rpm). The experimental set-up is shown in Fig. 5.

The first group of results (impulse-type excited measurement data) was utilised to determine the reverberation time T_{20}, in accordance with the procedure specified in the standard ISO 3382-2:2010. This standard states that the reverberation time T_{20} is to be determined from the average slope of the energy decay curve obtained from part of the decay curve between −5 dB and −25 dB. The values obtained for three analysed frequencies are given in Table 2. The acoustic energy decay levels for the octave band with the central frequency of 125 Hz, 250 Hz and 500 Hz are shown in Figs. 6–8.

Table 2. Reverberation time T_{20} for the given octave bands.

T_{20} [s]	125 [Hz]	250 [Hz]	500 [Hz]
	0.395	0.161	0.160

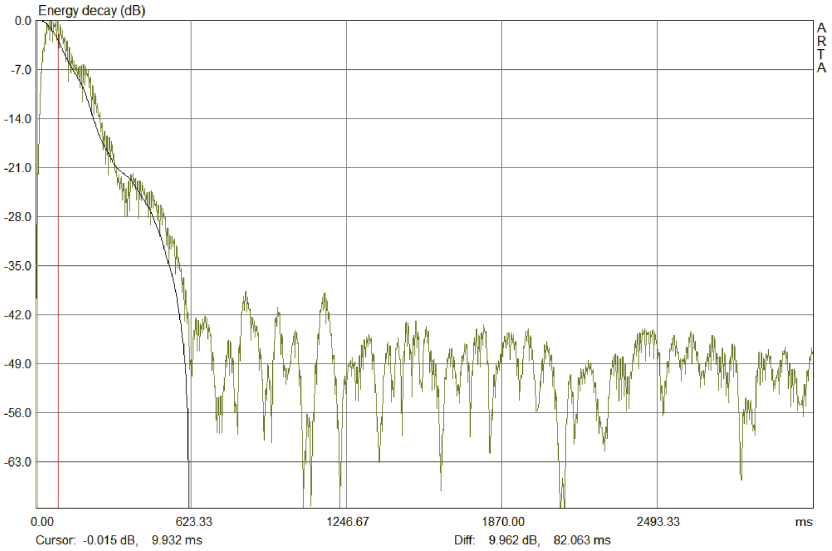

Fig. 6. Energy decay for an octave band with the central frequency 125 Hz.

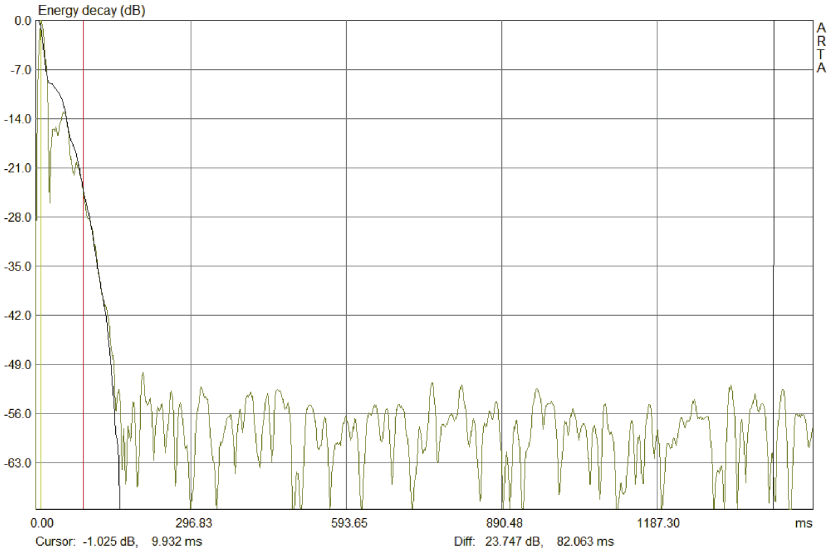

Fig. 7. Energy decay for an octave band with the central frequency 250 Hz.

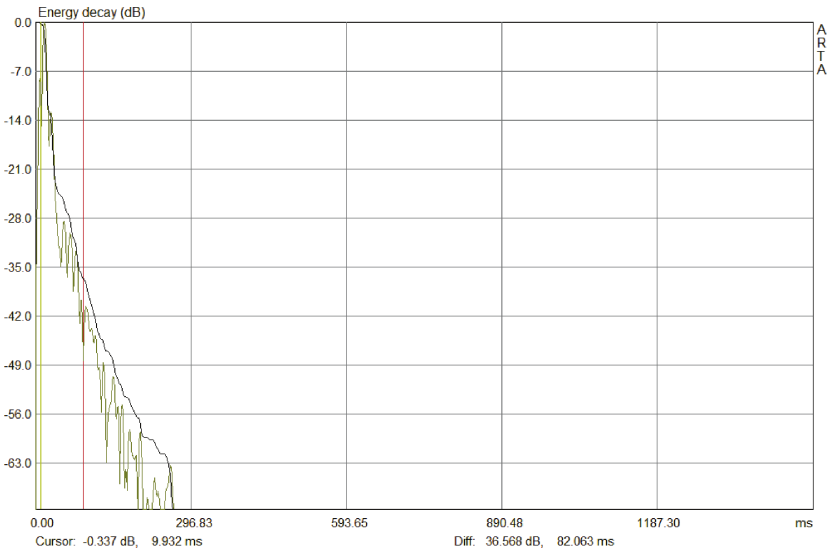

Fig. 8. Energy decay for an octave band with the central frequency 500 Hz.

During measurements of impulse response for acoustic type of excitation the starting pistol shot was used. The measurements were made for a number of microphone positions (eg. in the corners of the cabin and in the place of the head operator). In this paper are presented sonograms for microphone positioned in the cab corner in front of cab wall (Fig. 9) and the rear of the cab wall (Fig. 10).

Spectral analysis of the acoustic pressure response was performed for three rotational speeds of the engine (idle run) – about 750 rpm, 1600 rpm and 2300 rpm. A sonogram (Fig. 9) for the investigated volume obtained with the use of the programme REW v.5.0 shows the resonance at about 163 Hz. This figure also presents resonance at about 112 Hz, however it does not correspond to any calculated value of resonant frequency. It is probably due to not cuboid shape of the realistic cab. Figure 10 gives the sonogram revealing the resonance effect at about 397 Hz.

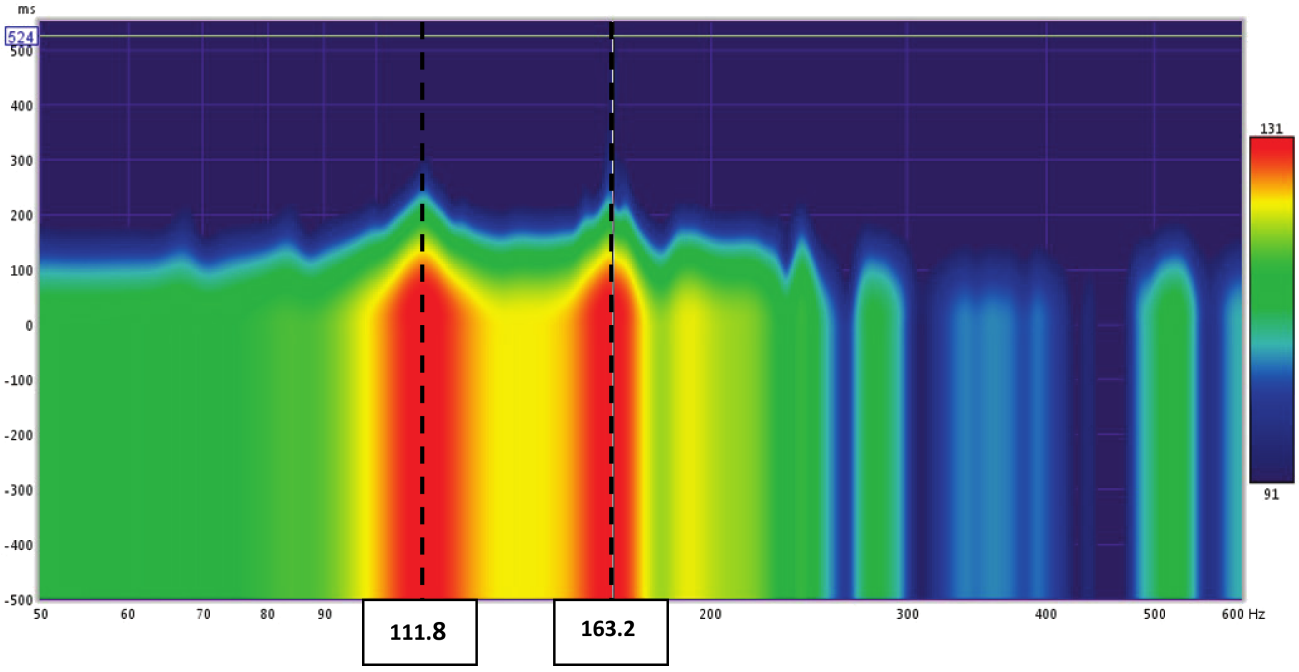

Fig. 9. Sonogram revealing the resonance at about 163 Hz.

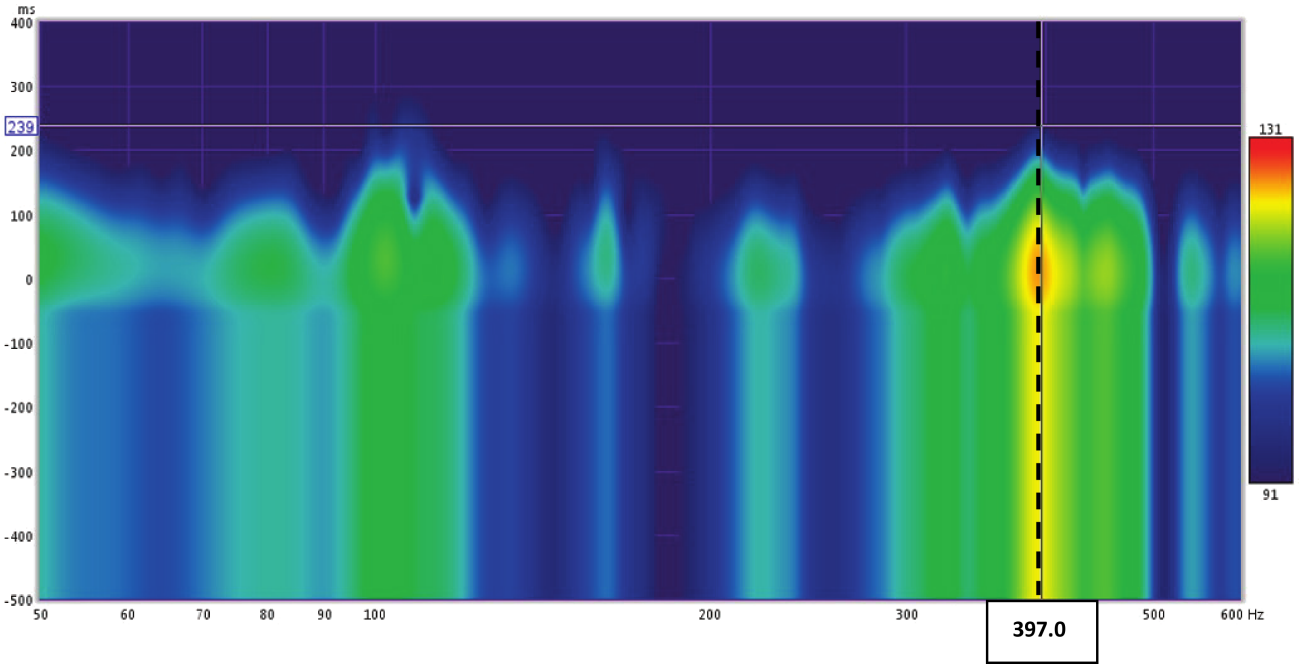

Fig. 10. Sonogram revealing the resonance at about 397 Hz.

During the measurement process the sound pressure level spectra in the cab were measured for the rotational speed of the engine: 750 rpm, 1600 rpm, 2300 rpm. Sound pressure distributions for rotational speeds 750 rpm, 1600 rpm, 2300 rpm are shown in Figs. 11, 12 and 13.

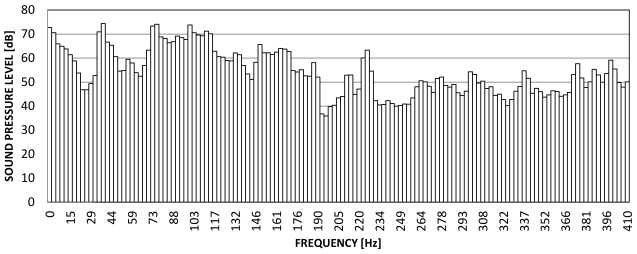

Fig. 11. Sound pressure level at 750 rpm.

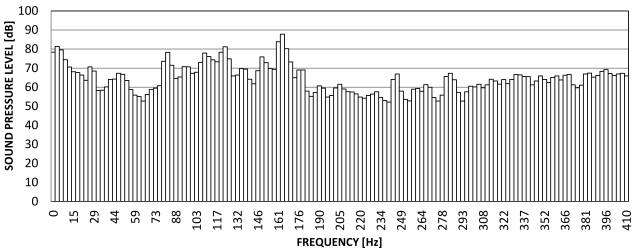

Fig. 12. Sound pressure level at 1600 rpm.

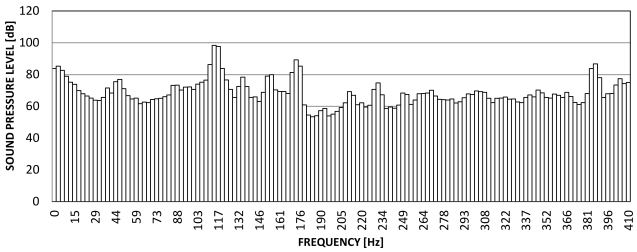

Fig. 13. Sound pressure level at 2300 rpm.

4. Source identification of acoustic frequencies

4.1. Engine components

The identification procedure takes into account the following frequencies: due to rotational speeds ones, according to valve ones (1) and connected with ignition ones (2), where $k = 1, 2, 3, \ldots$, z_V – number of valves, z_I – number of cylinders, s – stroke coefficient (four-stroke engine: $s = 0.5$), f_0 – frequency of shaft rotation.

$$f_V = kz_V f_0 s, \tag{1}$$

$$f_I = kz_I f_0 s. \tag{2}$$

Identified spectral components of rotation, valve and ignition frequencies are compiled in Table 3 and Table 4 (Dziechciowski, Kozień, 2014b).

Table 3. Identification of rotation, valve and ignition frequencies at 750 rpm (in the frequency range up to 400 Hz).

Frequencies [Hz]		Measured acoustic pressure level [dB]	Frequencies [Hz]		Measured acoustic pressure level [dB]	Frequencies [Hz]		Measured acoustic pressure level [dB]
Rotation calculated	Rotation measured		Valve calculated	Valve measured		Ignition measured	Ignition measured	
12.5	12	63.8	37.5	38	74.4	150	152	62.2
25	26	46.8	75	76	74.1	300	299	54.3
37.5	38	74.4	112.5	111	71.2	450	451	47.7
50	50	54.6	150	149	65.7			
62.5	62	53.9	187.5	188	58.1			
75	76	74.1	225	226	63.3			
87.5	88	66.8	262.5	164	64			
100	100	73.8	300	299	54.3			
112.5	111	71.2	337.5	337	54.7			
125	126	59	375	375	57.7			
137.5	135	61.4	412.5	413	53.1			
150	149	65.7						
162.5	164	64						
175	176	54.2						
187.5	188	58.1						
200	202	40.4						
212.5	211	52.9						
225	226	63.3						
237.5	240	42.3						
250	252	40.9						

Table 4. Identification of rotation, valve and ignition frequencies at 2300 rpm (in the frequency range up to 400 Hz).

Frequencies [Hz]		Measured acoustic pressure level [dB]	Frequencies [Hz]		Measured acoustic pressure level [dB]	Frequencies [Hz]		Measured acoustic pressure level [dB]
Rotation calculated	Rotation measured		Valve calculated	Valve measured		Ignition measured	Ignition measured	
38.3	38	71.5	115	114	98.4	460	463	68.6
76.7	76	65	230	231	74.7			
115.0	114	98.4	345	346	70.3			
153.3	155	79.9	460	463	68.6			
191.7	193	58.6						
230.0	231	74.7						
268.3	270	70.1						
306.7	308	68.9						
345.0	346	70.3						
383.3	387	86.7						
421.7	425	67.1						

Internal resonant acoustic frequency of the cab is given as:

$$f_a = 0.5 \cdot c \cdot \sqrt{\left(\frac{l^2}{h^2}\right)^2 + \left(\frac{m^2}{b^2}\right)^2 + \left(\frac{n^2}{d^2}\right)^2}, \qquad (3)$$

where l, m, $n = 1, 2, 3, \ldots$, c is the speed of sound; b, d, h are the respective dimensions (length, width and height) of a rectangular cab.

The measurements of the impulse response of the cab interior are well utilised in the analysis. The formula (3) is recalled to determine the relevant frequencies for the axial, tangent and oblique modes. Identified resonant acoustic frequencies are compiled in Table 5 and Table 6 (Dziechciowski, Kozień, 2014b). Identification was based on comparison of theoretically calculated values of resonance frequency and values of frequency occurring in noise spectrum measured inside the cab during engine operation.

Results of impulse response measurements shown in the form of sonograms in Fig. 9 and Fig. 10 reveal that the acoustic resonance within the investigated volume occurs at about 163 Hz and 397 Hz. Calculated data compiled in Table 5 and Table 6 suggest that these frequencies are associated with the axial modes that originate inside the cab. The measurements of the sound pressure spectra at varying engine speeds provide the preliminary information about the effects that wave phenomena can have on noise levels within the investigated volume.

Table 5. Identification of resonant acoustic frequencies at 750 rpm (in the frequency range up to 400 Hz).

Frequencies [Hz]		Measured acoustic pressure level [dB]	Frequencies [Hz]		Measured acoustic pressure level [dB]	Frequencies [Hz]		Measured acoustic pressure level [dB]
Axial theoretical	Axial measured		Tangent theoretical	Tangent measured		Oblique theoretical	Oblique measured	
132.3	132	62.1	208.2	208	44.0	264.9	264	50.5
160.7	161	62.5	210.6	211	52.9	350.3	346	47.4
163.8	164	64.0	229.5	229	54.6	384.3	384	50.1
264.6	264	50.5	309.6	308	50.4	388.2	387	55.3
321.5	319	45.0	311.2	311	47.3	447.5	448	45.7
327.6	328	42.8	347.7	346	47.4	450.8	451	47.7
396.9	398	59.1	353.3	349	46.0	458.5	457	47.9
482.2	480	43.9	360.8	360	46.1	477.7	480	43.9
			364.9	366	44.7			
			416.4	413	53.1			
			421.1	422	47.9			
			428.2	428	50.0			
			429.4	431	49.8			
			459	463	47.4			

Table 6. Identification of resonant acoustic frequencies at 2300 rpm (in the frequency range up to 400 Hz).

Frequencies [Hz]		Measured acoustic pressure level [dB]	Frequencies [Hz]		Measured acoustic pressure level [dB]	Frequencies [Hz]		Measured acoustic pressure level [dB]
Axial theoretical	Axial measured		Tangent theoretical	Tangent measured		Oblique theoretical	Oblique measured	
132.3	132	72.5	208.2	208	62.2	264.9	264	68.1
160.7	161	69.4	210.6	211	69.3	350.3	346	70.3
163.8	164	69.4	229.5	229	70.7	384.3	384	83.8
264.6	264	68.1	309.6	308	68.9	388.2	387	86.7
321.5	322	65.8	311.2	311	65.0	447.5	448	55.0
327.6	328	64.6	347.7	346	70.3	450.8	451	53.3
396.9	398	68.1	353.3	349	68.5	458.5	457	55.3
482.2	480	63.4	360.8	360	67.0	477.7	480	63.4
			364.9	366	68.8			
			416.4	413	68.7			
			421.1	422	66.6			
			428.2	431	63.5			
			429.4	434	63.5			
			459.0	463	68.6			

4.2. Structural wall modes

There is no accurate analytical solution to the problem of natural vibration of polygon – shaped panels with their edges clamped, therefore the analysis of natural vibrations of wall elements in the cab relied on the FEM approach, and the calculation procedure was supported by the *Ansys* package.

An assumption was made that cab walls should be modelled as independently vibrating thin Kirchhoff plates, in consideration of the manner they were fixed. The cab walls are either welded or bolted to one another and this connection is modelled as clamped. Furthermore, it was assumed that in the case of side walls incorporating glazed windows, they are fixed rigid enough so that the entire modelled element should be treated as a whole in the FEM procedure and care should be just taken into account for the presence of different materials in different wall sections. In consideration of the engineering design and construction of the wall elements, not all panel elements were subjected to the modal analysis. Some of them are structured like ribbed plates and a simple model of boundary conditions for the cab door is unavailable.

The description of investigated panels is provided in Table 7. Properties of structural materials are:

- for steel:
  - density 7800 kg/m^3,
  - Young modulus 210 GPa,
  - Poisson ratio 0.29;
- for glass:
  - density 2300 kg/m^3,
  - Young modulus 62 GPa,
  - Poisson ratio 0.27.

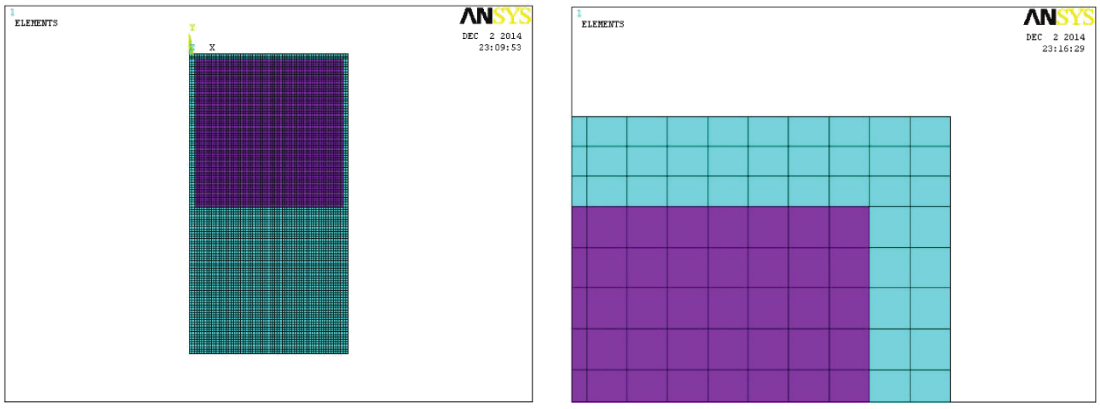

Fig. 14. FEM mesh for front panel (left – whole panel, right – corner).

Table 7. Description of investigated panels.

Panel ID.	Description	Plate(s) No.
A	Floor plate 1	1
B	Floor plate 2	2
C	Back plate	3
D	Roof door	5
E	Front panel	9, 10
F	Right wall	–

No damping is assumed for modal analysis. The elastic shell element shell63 (Ansys) is used in analysis. Maximal length of the side of quadrilateral finite element does not exceed 0.1 m. Example of meshed front panel is shown in Fig. 14.

Table 8 summarises the lowest natural frequencies for particular panels and the corresponding frequencies identified in the acoustic pressure spectrum in the low frequency range.

Table 8. Identification of structural acoustic frequencies of the cab for the rotational speed of the engine 2300 rpm (in the range up to 500 Hz).

Mode No.	Element ID.											
	A		B		C		D		E		F	
	FEM	MEAS.	FEM	MEAS.	FEM	MEAS.	FEM	MEAS.	FEM	MEAS.	FEM	MEAS.
1	114.5	111.3	593.0	591	33.2	38.1	255.9	–	151.9	149.4	114.5	111.3
2	201.6	202.2			63.5	67.4	520.9	527.3	210.8	213.9	201.6	202.2
3	261.8	266.6			71.5	76.1			289.8	290	261.8	266.6
4	341.1	339.8			99.4	99.6			391.6	389.6	341.1	339.8
5	342.9	342.7			111.6	111.3			431.6	430.7	342.9	342.7
6	474.6	475.5			130.8	134.8			457.5	457	474.6	475.5
7	486.3	483.4			145.5	149.4			526.6	527.3	486.3	483.4
8	534.8	539			157.2	164.0					534.8	539
9					176.5	178.7						
10					201.4	202.2						
11					209.0	208.0						
12					210.1	213.9						
13					235.6	240.2						
14					257.8	260.7						
15					263.2	266.6						
16					278.3	278.3						
17					289.4	–						
18					309.2	313.5						
19					334.1	336.9						
20					338.5	339.8						
21					342.0	342.8						
22					355.5	357.4						
23					375.8	375.0						
24					386.3	386.7						
25					415.7	413.1						
26					428.2	424.8						
27					434.3	430.6						
28					437.8	433.6						
29					452.5	451.1						
30					469.5	–						
31					493.3	495.1						
32					499.6	501.0						
33					509.7	509.8						
34					510.0	–						

5. Final remarks

In the light of the underlying assumptions that identification of acoustic frequency of the cab should involve major simplifications as to actual shape of the cab (acoustic volume), that cab walls should be modelled as single panels with the clamp-type boundary condition, and that frequencies of the rotating motion, of the valve and of the ignition can be derived from simple formulas, it appears that most acoustic frequencies in the operator's cab were identified with a relatively low error levels.

The employed identification method allows for connecting the spectral components of the engine-type source with the relevant resonant acoustic ones. Some of these components are of structural type (bending vibrations of panels-cab walls). They were successfully identified for most considered modes, even though the FEM procedure relied on a simplified model of the cab wall structure.

The obtained values of reverberation time suggest that the internal acoustic parameters of the cab can be altered through internal noise reduction by acoustic damping.

References

1. Carletti E. (2013), *A perception based method for the noise control of construction machines*, Archives of Acoustics, **38**, 2, 253–248.
2. Chiu M.-C. (2013), *Noise elimination of a multi-tone broadband noise with hybrid Helmholtz mufflers using a simulated annealing method*, Archives of Acoustics, **37**, 4, 489–498.
3. Cempel Cz. (1989), *Applied vibroacoustics* [in Polish: *Wibroakustyka stosowana*], PWN, Warszawa.
4. Dziechciowski Z., Kozień M.S. (2014a), *Experimental investigation of acoustic parameters for machine cabine*, Proceedings of the Colloquium Dynamics of Machines, Prague, 35–40.
5. Dziechciowski Z., Kozień M.S. (2014b), *Identification of experimentally measured acoustic modes inside bulldozer cabine*, CD Proceedings of the Forum Acusticum, Cracow, ISSN-2221-3767, 6 pages.
6. Dziechciowski Z., Stolarski B., Wiciak J. (2001), *Sound transmission loss computation of a gantry crane cab* [in Polish: *Ocena izolacyjności kabin suwnic bramowych*], Engineering Machine Problems, **18**, 133–141.
7. Engel Z. (2001), *Protecting the environment against vibration and noise* [in Polish: *Ochrona środowiska przed drganiami i hałasem*], PWN, Warszawa.
8. Freymann R. (1999), *Acoustic applications in vehicle engineering* [in:] *Fluid-structure interaction in acoustics*, Habaut D. [Ed.], International Centre for Mechanical Sciences – Courses and Lectures No. 396, Springer-Verlag, Wien-New York.
9. Hargreaves J.A. (1998), *The use of indirect coupled boundary element analysis in vehicle NVH refinement*, Proceedings of IMechE, C521/019, 213–227.
10. ISO 3382-2:2010, *Acoustics – Measurement of Room Acoustic Parameters – Part 2: Reverberation Time in Ordinary Rooms*.
11. Kazimierska M., Grębosz M. (2001), *The level of noise emission by the working machines with references to European and Polish standards* [in Polish: *Poziom hałasu emitowanego przez maszyny robocze w odniesieniu do norm Unii Europejskiej i Polskich Norm*], Engineering Machine Problems, **17**, 127–134.
12. Koopman G.L. (1982), *Interior noise in transportation vehicles* [in:] *Noise generation and control in mechanical engineering*, Davies P.O.A.L., Heckl M., Koopman G.L. [Eds.], International Centre for Mechanical Sciences – Courses and Lectures No. 276, Springer-Verlag, Wien-New York.
13. Kozień M.S., Nizioł J. (1993), *Reduction of the values of the normal surface velocity for vibrating glass of the bulldozer TD20E* [in Polish: *Zmniejszenie wartości prędkości normalnej dla drgań szyby przedniej spycharki TD20E – analiza teoretyczna*], Technical Bulletin of Rzeszow University of Technology – Mechanics, **117**, 38, 71–78.
14. Kozień M.S., Wiciak J. (2004), *Analysis of noise radiated by structural elements of operators' cab* [in Polish: *Ocena hałasu emitowanego przez elementy poszycia kabin maszyn roboczych*], Engineering Machine Problems, **23**, 79–90.
15. Kozień M.S., Wiciak J. (2004), *Changing of thickness of operator's cab as a method of increasing of the acoustic comfort of their operators*, Polish Journal of Environmental Studies, **13**, (Suppl. III), 110–113.
16. Kozień M.S., Wiciak J. (2008), *Reduction of structural noise inside crane cage by piezoelectric actuators – FEM simulation*, Archives of Acoustics, **33**, 4, 643–652.
17. Kozień M.S., Wiciak J. (2009), *Choosing of optimal voltage amplitude of four pairs square piezoelectric elements for minimization of acoustic radiation of vibrating plate*, Acta Physica Polonica A, **A 116**, 3, 348–350.
18. Kozień M.S., Wiciak J. (2010), *Passive structural acoustic control of the smart plate – FEM simulation*, Acta Physica Polonica A, **118**, 6, 1186–1188.
19. Michałowski S. (1999), *State of investigations on the field of vibration and noise reduction in heavy duty machine cabs* [in Polish: *Stan badań związanych z redukcją drgań i hałasu w maszynach roboczych ciężkich*], Engineering Machine Problems, **14**, 55–85.
20. Michałowski S., Stolarski B. (1998), *Vibration and noise control in heavy duty machines* [in Polish: *Zwalczanie wibracji i hałasu w maszynach roboczych ciężkich*], Monography, Cracow University of Technology, Cracow.
21. Min S., Nagamura K., Nakagawa N., Okamura M. (2013), *Design of compact micro-perforated membrane absorbers for polycarbonate pane in automobile*, Applied Acoustics, **74**, 622–627.

22. Misun S., Svancara P. (2001), *Acoustic properties of the tractor cabin solved by using SEA method*, Proceedings of the Eighth International Congress on Sound and Vibration, Hong Kong, 2335–2342.

23. Myung-Ho S., Jang-Moo L., Seock-Hyun K., Dong-Chul P., Seung-Gyun Ch., Jung-Hee K. (1993), *A study on the vibration and acoustic characteristics of a passenger car*, Proceedings of Asia-Pacific Vibration Conference, Kitakyushu, 694–699.

24. Nefske D.J., Wolf J.A., Howell J.R. (1982), *Structural acoustic finite element analysis of the automotive passenger compartment. A review of current practice*, Journal of Sound and Vibration, **80**, 2, 247–266.

25. Nelson P.A., Elliott S.P. (1993), *Active control of sound*, Academic Press Ltd.

26. Nizioł J. (Ed.) (1987), *Reduction of vibration noise for cages of caterpillar bulldozer* [in Polish: *Obniżenie wibracji i hałasu w kabinach spycharek gąsienicowych*], Technical Note for the Stalowa Wola Steelworks HSW, Cracow University of Technology, Kraków.

27. Pleban D. (2014), *Definition and measurement of the sound quality of the machine*, Archives of Acoustics, **39**, 1, 17–23.

28. Rdzanek W.P. (2002), *The sound pressure from an individual mode of a clamped-free annular plate*, Archives of Acoustics, **27**, 2, 147–155.

29. Rdzanek W.P., Engel Z., Rdzanek W. (2003), *Theoretical analysis of sound radiation of an elastically supported circular plate*, Journal of Sound and Vibration, **265**, 1, 155–174.

30. Stoebener U., Gaul L. (2001), *Active vibration control of a car body based on experimentally evaluated modal parameters*, Mechanical Systems and Signal Processing, **15**, 1, 173–188.

31. Stolarski B. (1995), *Application of noise reduction method in heavy duty machines cabins*, Proceedings of the Conference on Noise Control Engineering, Warsaw, 459–466.

32. Succi G.P. (1987), *The interior acoustic field of an automobile cabin*, J. Acoust. Soc. Am., **81**, 6, 1688–1694.

33. Sung-Hee K., Suk-Yoon H., Jee-Hun S., Won-Ho J. (2012), *Interior noise analysis of a construction equipment cabin based on airborne and structural-borne predictions*, Journal of Mechanical Science and Technology, **26**, 4, 1003–1009.

34. Szemela K., Rdzanek W.P., Rdzanek W.J. (2013), *Acoustic power radiated by a system of two vibrating circular membranes located at the boundary of three-wall corner spatial region*, Archives of Acoustics, **37**, 4, 463–473.

35. Turner W.B., Turgay F.M. (1998), *Development of coupled structure – acoustic FE models for vehicle refinement*, Proceedings of IMechE, C521/026, 229–238.

36. Xiaofeng S., Ming M., Junfang W. (2012), *Effect of a low Mach number flow on a semi active Helmholtz resonator*, CD Proceedings of the 19th International Conference on Sound and Vibration ICSV19, Vilinus, 5 pages.

37. Zawieska W.M., Rdzanek W.P. (2006), *Low frequency approximation of natural modal radiation efficiency of some simply supported flat plates*, Archives of Acoustics, **31**, 4, 123–130.

38. Zawieska W.M., Rdzanek W.P., Rdzanek W., Engel Z. (2007), *Low frequency estimation for the sound radiation efficiency of some simply supported flat plates*, ActaAcustica united with Acustica, **93**, 3, 353–363.